# Nonlinear VIV Modelling and 3-D Response Properties over a Full Bridge Span

Zhitian Zhang [1]

[1]College of Civil Engineering and Architecture, Hainan University, Haikou, China, zhangzhitian@hainanu.edu.cn

**SUMMARY:**
Nonlinear vortex-induced vibration (VIV) performances of a bridge section are investigated in terms of motion amplitude ($y_T$) dependent energy-trapping properties. Energy-trapping properties of a model undergoing a full-process from still to a limit cycle oscillation (LCO) state are determined. Nonlinear parameter-amplitude relations are established. Aerodynamic damping during the VIV lock-in range is separated into the initial damping and the $\varepsilon$–related part which varies with both the reduced wind speed and the motion amplitude. The initial aerodynamic damping determines the threshold of VIV, while the $\varepsilon$–related part dominates the evolution process and the LCO. The identified nonlinear analytical model is capable of determining VIV responses at higher mechanical damping ratios. The energy-trapping properties of a section model in time-domain are transformed into nonlinear distribution properties in space along an elongated 3-D elastic bridge span. According to this "time-space" transformation, the convection coefficient, which links the maximum response of a 3-D structure with that of a 2-D sectional model can be determined. The nonlinear model presented reveals significantly larger convection coefficients than existing methods.

*Keywords: VIV; energy-trapping; Nonlinear; full-bridge*

## 1. NONLINEARIZED VIV MODEL

For structures being released to vibrate from still, the nonlinear aerodynamic damping ratio is assumed to be expressed with an initial term $\xi_{in}$ plus a motion dependent nonlinear term $\xi_{\varepsilon}$. Selection of an analytical model can be evaluated by its capability of reflecting the energy-trapping properties dominating the structure's motion evolution. It is noted that the motion evolution here includes not only the final LCO but also the intermediate process. Modelling the intermediate process entails observing the evolution of the macroscopic damping ratios (negative $\xi$), which evolves with the motion amplitude $y_T(t)$, and this should be reflected by the adopted analytical model. Once the evolution of $\xi$ with $y_T(t)$ is obtained, the energy-trapping/dissipating along a 3-D elastic full bridge span can be determined accordingly.
The equation of motion of a sectional model free to vibration is

$$m\ddot{y} + c\dot{y} + ky = F_{\mathrm{a}} \tag{1}$$

where m is the mass or mass moment of the model; c is the mechanical damping coefficient; k is the structural stiffness; y, $\dot{y}$, $\ddot{y}$ are structural displacement, velocity, and acceleration, respectively.

An existing model is altered slightly here for basic expression of $F_a$(Scanlan, 1981; Ehsan and Scanlan, 1990). The work done by the aerodynamic load $F_a$ during a single oscillation period has been determined to be

$$W_a = \frac{1}{2}\rho UDL\frac{Y_1\omega^2}{4\lambda}\left[y_T^2\left(e^{2\lambda T}-1\right)-\varepsilon y_T^4\frac{1}{8D^2}\left(e^{4\lambda T}-1\right)\right] \quad (2)$$

where ρ is the air density; U is wind speed; D is the reference height; L is the model length; $Y_1$ is a function of $U_r$; $U_r = U/Df$ is the reduced wind speed; $y_T$ is the transient motion amplitude; $\omega$ is the vibrating circular frequency; $\lambda = -\xi\omega$ is an exponential coefficient. $T$ is the motion period; ε is a model parameter to be identified that provides self-limiting property for the system. On the other hand, the negative work done by the mechanical damping force is

$$W_c = -cy_T^2\frac{\omega^2}{4\lambda}\left(e^{2\lambda T}-1\right) \quad (3)$$

According to (2) and (3), the link between $\varepsilon$ with the motion amplitude $y_T$ between is determined to be

$$\varepsilon(U_r, y_T) = \frac{8D^2}{y_T^2(e^{2\lambda T}+1)}\left[1+\frac{c}{c_{in}}\right]+\frac{\Delta W\cdot 32\lambda D^2}{c_{in}\omega^2 y_T^4(e^{4\lambda T}-1)} \quad (4)$$

This relation is able to be determined by a known time history similar to that shown in Fig. 1.
In a LCO state, $\Delta y = 0$, $\Delta W = 0$, $y_T = y_{lco}$ Therefore Eq. (4) becomes

$$\varepsilon_0 = \frac{4D^2}{y_{lco}}\left[1+\frac{c}{c_{ae}}\right] \quad (5)$$

where $y_{lco}$ is the LCO amplitude. $y_{lco}$ is a function of mechanical damping. Eq. (5) states that $\varepsilon$ in a LCO state, denoted here by $\varepsilon_0$, is jointly determined by the mechanical damping, the initial aerodynamic damping, and the final motion amplitude. The calculation of $\varepsilon$ by Eq. (4) or (5) implies $c_{in}$ being identified first, which can be determined by the foremost cycles of motion as

$$Y_1 = 2\frac{n\pi c - m\omega\delta_n}{n\pi\rho UDL} \quad (6)$$

The part of damping ratio contributed by the aerodynamic loading is determined to be

$$\xi_\varepsilon(U_r, y_T) = \rho UL\frac{Y_1\varepsilon y_T^2}{32m\omega D}\left(e^{2\lambda T}+1\right) \quad (7)$$

The most direct application of the above developed nonlinear model is the prediction of VIV responses at higher mechanical damping ratios, as shown in Figure 1.

## 2. PEAK RESPONSE OF A 3D BRIDGE SPAN

The governing equation of VIV motion based on a modal shape function can be given as

$$\ddot{q} + 2\xi_s\omega\dot{q} + \omega^2 q = \frac{\rho U^2 D}{2M_q}\int_0^L \varphi(x)\left[Y_1\left(1-\varepsilon(x)\frac{y^2}{D^2}\right)\frac{\dot{y}}{U}\right]dx \quad (8)$$

where $q$ is the generalized coordinate; $\varphi_v(x)$ is the modal shape function in the vertical direction. Adjusting Eq. (8) yields

$$\ddot{q} + \left\{2\xi_s\omega - \frac{\rho UDY_1}{2m_e} + \frac{\rho UY_1 q^2}{2m_e D}\cdot\frac{\int_0^L \varepsilon(x)\varphi_v^4(x)dx}{\int_0^L \varphi_v^2(x)dx}\right\}\dot{q} + \omega^2 q = 0 \quad (9)$$

The final solution of Eq. (9), can be determined by the energy balance principle. Supposing $q(t) = q_0 \sin(\omega t)$, the energy balance during a single motion cycle leads to

$$\int_0^{\frac{2\pi}{\omega}} \left\{ 2\xi_s\omega - \frac{\rho U D Y_1}{2m_e} + \frac{\rho U Y_1 q_0^2 \sin^2(\omega t)}{2m_e D} \cdot \frac{\int_0^L \varepsilon(x)\varphi_v^4(x)dx}{\int_0^L \varphi_v^2(x)dx} \right\} \omega \cos^2(\omega t)\, dt = 0 \tag{10}$$

Thus, the LCO amplitude, $q_0$, is obtained as

$$q_0 = \sqrt{\left(\frac{\rho U D Y_1}{2m_e} - 2\xi_s\omega\right)\frac{8m_e D}{\rho U Y_1} \cdot \frac{\int_0^L \varphi_v^2(x)dx}{\int_0^L \varepsilon(x)\varphi_v^4(x)dx}} \tag{11}$$

Eq. (11) is unable to be solved directly because not all parameters that appear on the right-hand side are determined, due to $\varepsilon(x)$ being dependent on the motion amplitude, namely $q_0|\varphi_v(x)|$. However, the motion amplitude at location $x$ is unknown since $q_0$ itself needs to be solved first. Therefore, an iteration method is required to obtain the final solution. Introducing $\beta_v$ as the ratio of the maximum response of the 3-D structure to that of the 2-D model, it can be determined as

$$\beta_v = \frac{q_0|\varphi_{v,max}(x)|}{y_0} = \lambda|\varphi_{v,max}(x)| \sqrt{\varepsilon_0 \frac{\int_0^L \varphi_v^2(x)dx}{\int_0^L \varepsilon(x)\varphi_v^4(x)dx}} \tag{12}$$

where $\lambda$ is the geometric scale. However, it is noted that $\lambda$ applies to transverse VIVs only, and its torsional response counterpart would always be irrelevant to the geometric scale.

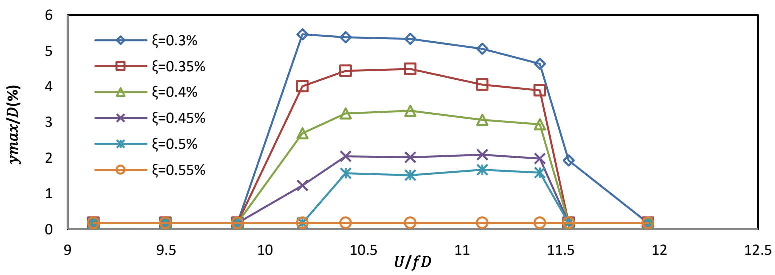


**Fig. 1** VIV motion amplitude predicted for higher mechanical damping ratios

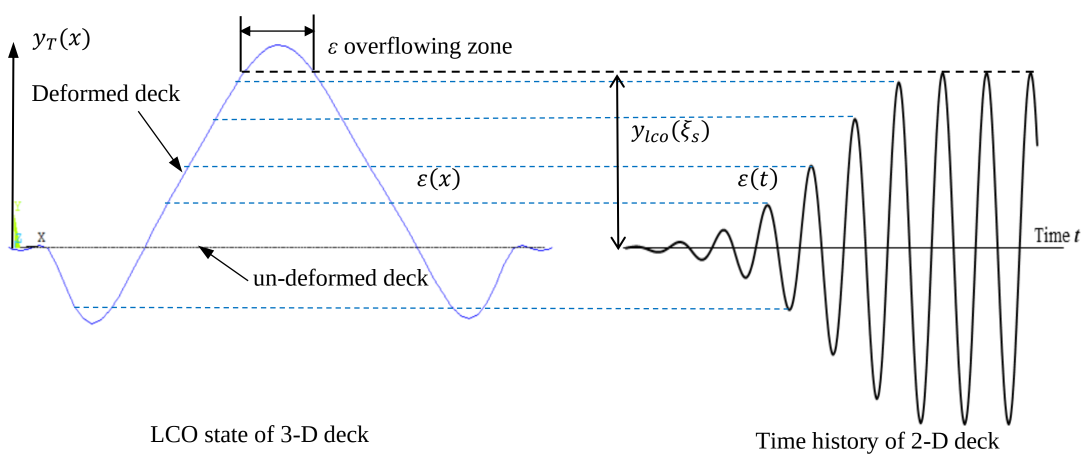


**Figure 2.** ‘Time-space’ transformation relationship between the 2-D and 3-D VIV responses

The overflowing phenomena has been observed (see Figure 2), and it indicates that, to predict the VIV response of a full bridge structure, the mechanical damping ratio $\xi_s$ used by the sectional model must be lower than the targeted value at least to some extent. Compared with the linear model (Zhang, et al., 2014) resulted $\beta_v$, 1.234, those based on the nonlinear model can be as large as 2.171 (see Table 1). It is worthy of noting that the mechanical damping in this study is viewed as a fixed value independent of the motion amplitude. Recent studies indicate, however, that the mechanical damping of both a section of a full-bridge model varies with motion amplitude (Tang and Hua, 2019; Xu et al., 2021; Li, et al, 2022). Therefore, a refined identification of the model parameters should take into account this property in the future.

**Table 1**. $\beta_v$ calculated from a nonlinear Van der Pol model

| $\xi_s$ \ $U_r$ | 10.19 | 10.41 | 10.74 | 11.1 | 11.39 |
|---|---|---|---|---|---|
| 0.003 | Overflowed | Overflowed | Overflowed | Overflowed | Overflowed |
| 0.004 | 1.314 | 1.315 | 1.293 | 1.373 | 1.393 |
| 0.005 | 1.893 | 1.381 | 1.397 | 1.957 | 2.171 |

## 3. CONCLUSIONS

The core mechanism of the proposed method is concerned with the relation between energy-trapping property and the motion amplitude, according to which a non-linear VIV model is established. The following conclusions are drawn:

1) The nonlinear $\varepsilon$–$y_T$ relation is established, which is able to predict the VIV responses of the model at higher mechanical damping ratios or to predict the maximum responses of the 3-D elastic bridge span.
2) Parameter overflowing could occur in a range of a 3-D bridge span when the global energy balance entails motion amplitudes being larger than the LCO amplitude of the 2-D model.
3) The convection coefficient varies with both the mechanical damping and the reduced wind speed. The current example shows that the coefficient can be as large as 2.171, which is substantially larger than the linear-model-based value of 1.234.

**REFERENCES**


Scanlan, R. H., 1981. On the state-of-the-art methods for calculations of flutter, vortex-induced and buffeting response of bridge structures. FHWA/RD-80/050, Nat. Tech. Information Service, Springfield, Va.

Ehsan, F., Scanlan, R. H., 1990. Vortex-induced vibrations of flexible bridges. ASCE Journal of Engineering Mechanics 116 (6): 1392-1411.

Li, Z., Wu, B., Liao, H., Li, M., Wang, Q., Shen, H., 2022. Influence of the initial amplitude on the flutter performance of a 2D section and 3D full bridge with a streamlined box girder. Journal of Wind Engineering & Industrial Aerodynamics 222: 104916.

Tang, Y., Hua, X., 2019. Experimental investigation of flutter characteristics of shallow Π section at post-critical regime. Journal of Fluids and Structures. 88, 275-291.

Xu, F., Yang, J., Zhang, M., Yu, H., 2021. Experimental investigations on post-flutter performance of a bridge deck sectional model using a novel testing device. Journal of Wind Engineering & Industrial Aerodynamics 217: 104752.

Zhang, Z., Ge, Y., Chen, Z., 2014. Vortex-induced oscillations of bridges: linkages between sectional model tests and full bridge responses, Wind and Structures 19(3): 233-247.